Fixed-Time Attitude Control for Rigid Spacecraft With Actuator Saturation and Faults

Boyan Jiang, Qinglei Hu, and Michael I. Friswell

***Abstract*— This brief investigates the finite-time control problem associated with attitude stabilization of a rigid spacecraft subject to external disturbance, actuator faults, and input saturation. More specifically, a novel fixed-time sliding mode surface is developed, and the settling time of the defined surface is shown to be independent of the initial conditions of the system. Then, a finite-time controller is derived to guarantee that the closed-loop system is stable in the sense of the fixed-time concept. The actuator-magnitude constraints are rigorously enforced and the attitude of the rigid spacecraft converges to the equilibrium in a finite time even in the presence of external disturbances and actuator faults. Numerical simulations illustrate the spacecraft performance obtained using the proposed controller.**

***Index Terms*— Actuator faults, attitude control, fixed-time control, input saturation, spacecraft.**

I. Introduction

FUTURE spacecraft will be expected to ensure rapid, accurate, and global response to various attitude maneuvering commands. Furthermore, such a response should be achieved globally in the presence of large environmental disturbances, large uncertainties, subsystem and component failures, and even control input saturation. However, most of the existing research only considers uncertainties and assumes that faults or failures on the spacecraft system components will never occur. This assumption is rarely satisfied in practice because catastrophic faults may occur due to various malfunctions, especially in the actuators. If the attitude controller does not have any fault tolerance capability, severe performance degradation and system instability would result in the failure of the mission. Hence, research into fault-tolerant controllers has received considerable attention over the last decade [1]–[3].

Besides the obvious interest in ensuring closed-loop stability with fault-tolerant control, there is also a practical motivation in introducing saturation nested within the control loop. In practice, because of physical limitations, the outputs of momentum exchange devices and/or thrusters are constrained. A common example of such a constraint is actuator saturation, which can lead to serious discrepancies between the commanded input signals and the actual control effort. When the actuator has reached its input limit, any effort to further increase the actuator output would result in no variation in the output, which may lead to system instability. Hence, the problem of actuator saturation is another critical issue that needs to be tackled and many research results have been obtained [4]–[7].

Although spacecraft attitude control can be met by using existing control designs, even under the effect of actuator faults and input saturation, almost all of the previously discussed control schemes require infinite time to accomplish an attitude maneuver. Obviously, such an infinite settling time is not an option during highly critical mission phases. Finite-time control techniques can provide a faster convergence rate, higher precision control performance, and better disturbance rejection properties. Existing finite-time control methods can be broadly classified into two categories: 1) the homogeneous domination approach [8], [9] and 2) the Lyapunov-based approach [10]. Unfortunately, the homogeneous approach cannot adjust or even estimate the settling time and the exact mathematical model of the spacecraft system should be known in advance. To overcome this limitation, finite-time controllers [11]–[14] based on the Lyapunov approach have been designed for rigid spacecraft, and some of them can deal with actuator faults [12]–[14] or actuator saturation [13], [14].

Although there are fruitful results on Lyapunov-based finite-time approaches for attitude stabilization control of spacecraft, the initial system state must be known to estimate the settling time. In the initial design of the control system, it would be very helpful if the settling time could be predicted without requiring knowledge of the initial conditions. Thus, in contrast to existing finite-time controllers, the upper bound of the settling time could be estimated independent of initial conditions, in the sense of the fixed-time stability concept [15]. Inspired by the fixed-time-based finite-time convergence of the attitude system, this brief investigates the feasibility of attitude stabilization control in the presence of actuator faults, input saturation constraints, and even external disturbances, by employing adaptive nonlinear control techniques implemented using fixed-time-based finite-time control. The main contributions of this brief relative to most of the existing finite-time attitude controllers are the following two aspects. First, a new fixed-time-based terminal sliding mode (TSM), which explicitly contains $\boldsymbol{\omega}$, is given for the attitude system, and a complete proof of finite-time convergence is provided for the system states on the TSM. Second, an adaptive fixed-time-based finite-time attitude controller is designed that can guarantee finite-time reachability of the attitude orientation into a small neighborhood of the equilibrium point independent of

Manuscript received December 11, 2014; revised March 11, 2015 and October 19, 2015; accepted January 10, 2016. Date of publication February 3, 2016; date of current version August 4, 2016. Manuscript received in final form January 16, 2015. Recommended by Associate Editor B. Jiang.

B. Jiang is with the Department of Control Science and Engineering, Harbin Institute of Technology, Harbin 150001, China (e-mail: boyanjiang_hit@163.com).

Q. Hu is with the School of Automation Science and Electrical Engineering, Beihang University, Beijing 100191, China (e-mail: huql_buaa@buaa.edu.cn).

M. I. Friswell is with the College of Engineering, Swansea University, Swansea SA1 8EN, U.K. (e-mail: m.i.friswell@swansea.ac.uk).

Color versions of one or more of the figures in this paper are available online at http://ieeexplore.ieee.org.

Digital Object Identifier 10.1109/TCST.2016.2519838

1063-6536 © 2016 IEEE. Personal use is permitted, but republication/redistribution requires IEEE permission.
See http://www.ieee.org/publications_standards/publications/rights/index.html for more information.

Authorized licensed use limited to: CHONGQING UNIVERSITY. Downloaded on May 15,2023 at 10:16:32 UTC from IEEE Xplore. Restrictions apply.

the initial system state, by simultaneously considering external disturbances, actuator saturation, and faults.

Notation: Throughout this brief, we use $\|\cdot\|$ for the Euclidean norm of vectors and the induced norm for matrices. For a given vector $\boldsymbol{x} = [x_1, x_2, x_3]^T \in R^3$, define $\boldsymbol{x}^\alpha = [x_1^\alpha, x_2^\alpha, x_3^\alpha]^T$, $\text{sgn}(\boldsymbol{x}) = [\text{sgn}(x_1), \text{sgn}(x_2), \text{sgn}(x_3)]^T$, and $\text{sgn}(\boldsymbol{x})^\alpha = [|x_1|^\alpha \text{sgn}(x_1), |x_2|^\alpha \text{sgn}(x_2), |x_3|^\alpha \text{sgn}(x_3)]^T$, where $\alpha \in \mathbb{R}$ and $\text{sgn}(\cdot)$ denotes the sign function.

II. Background and Preliminaries

A. Spacecraft Attitude Dynamics

Consider a rigid spacecraft mathematical model with actuator faults and saturation as follows:

$$\begin{cases} \dot{q}_0 = -\dfrac{1}{2}\boldsymbol{q}^T\boldsymbol{\omega}, \qquad \dot{\boldsymbol{q}} = \boldsymbol{Q}(\boldsymbol{q})\boldsymbol{\omega} \\ \boldsymbol{J}\dot{\boldsymbol{\omega}} = -\boldsymbol{\omega}^\times \boldsymbol{J}\boldsymbol{\omega} + \boldsymbol{D}(\boldsymbol{I}-\boldsymbol{E})\text{sat}(\boldsymbol{u}) + \boldsymbol{D}\boldsymbol{E}\bar{\boldsymbol{u}} + \boldsymbol{d}(t) \end{cases} \tag{1}$$

where $[q_0, \boldsymbol{q}^T]^T \in \mathbb{R}^4$ represents the attitude orientation of the spacecraft, $\boldsymbol{\omega} \in \mathbb{R}^3$ denotes the angular velocity vector of the body-fixed reference frame of a spacecraft with respect to an inertial reference frame expressed in the body-fixed reference frame, $\boldsymbol{J} = \boldsymbol{J}^T \in \mathbb{R}^{3\times 3}$ denotes the positive definite inertia matrix of the spacecraft, and $\boldsymbol{Q}(\boldsymbol{q}) \in \mathbb{R}^{3\times 3}$ is defined as $\boldsymbol{Q}(\boldsymbol{q}) = (1/2)(q_0\boldsymbol{I} + \boldsymbol{q}^\times)$. Note that for any vector $\boldsymbol{a} = [a_1, a_2, a_3]^T$, the notation $\boldsymbol{a}^\times$ is used to denote the skew-symmetric matrix $\boldsymbol{a}^\times = [0, -a_3, a_2; a_3, 0, -a_1; -a_2, a_1, 0]$. Furthermore, $\boldsymbol{D} \in \mathbb{R}^{3\times m}$ is the actuator configuration matrix, m is the number of actuators, $\boldsymbol{u} \in \mathbb{R}^m$ denotes the desired control torque produced by the controller, and $\boldsymbol{I}$ represents the identity matrix with proper dimensions. $\boldsymbol{E} = \text{diag}(E_1, E_2 \ldots E_m) \in \mathbb{R}^{m\times m}$, where E_i denotes the failure indicator for the ith actuator. Note that the case $E_i = 0$ means that the ith actuator works normally. If $E_i = 1$, the ith actuator has failed completely without any control torque supplied. $E_i \in (0, 1)$ corresponds to the case in which the ith actuator has partially lost its effectiveness, but still works all of the time. $\bar{\boldsymbol{u}} \in \mathbb{R}^m$ represents uncertain failures in the actuators. Note that the presented fault model in (1) can represent outage, loss of effectiveness, and stuck faults. $\text{sat}(u_i)$ denotes the nonlinear saturation characteristic of the ith actuator and is of the form $\text{sat}(u_i) = \text{sgn}(u_i)\cdot\min\{|u|, |u_{\max,i}|\}$, where $u_{\max,i}$ is the maximum value of the ith entry of the control vector. Furthermore, the saturation function $\text{sat}(\boldsymbol{u})$ in (1) can be rewritten as $\text{sat}(\boldsymbol{u}) = \Theta(\boldsymbol{u})\cdot\boldsymbol{u}$ with $\Theta(\boldsymbol{u}) = \text{diag}(\Theta_1(u_1), \Theta_2(u_2) \ldots \Theta_m(u_m))$ and

$$\Theta_i(u_i) = \begin{cases} 1, & |u_i| \le u_{\max,i} \\ \text{sgn}(u_i)\cdot u_{\max,i}/u_i, & |u_i| > u_{\max,i} \end{cases} \quad i = 1, 2 \ldots m. \tag{2}$$

The coefficient $\Theta_i(u_i)$ may be considered as an indicator of the saturation degree of the ith entry of the control vector. From a practical point of view, $\boldsymbol{u}$ is never infinite as it is derived from a finite vehicle response, even if the upper bound for $\boldsymbol{u}$ can only be estimated. Hence, $\Theta_i(u_i)$ will never be zero, and a lower bound of $\Theta_i(u_i)$ exists. Thus, $\Theta_i(u_i) \in (0, 1]$ and there exists a constant δ satisfying $0 < \delta \le \min\{\Theta_1(u_1), \Theta_2(u_2) \ldots \Theta_m(u_m)\} \le 1$ [7]. In addition, $\boldsymbol{d} \in \mathbb{R}^3$ denotes the external disturbance torque vector.

B. Definitions and Lemmas

Consider the system

$$\dot{\boldsymbol{x}}(t) = \boldsymbol{f}(\boldsymbol{x}(t)), \quad \boldsymbol{x}(0) = \boldsymbol{0}, \quad \boldsymbol{f}(\boldsymbol{0}) = \boldsymbol{0}, \quad \boldsymbol{x} \in \mathbb{R}^n \tag{3}$$

where $\boldsymbol{f} : U_0 \to \mathbb{R}^n$ is continuous in an open neighborhood U_0 of the origin. Suppose that the system in (3) possesses a unique solution in forward time for all initial conditions.

Lemma 1 [15], [16]: Consider the nonlinear system in (3). Suppose that there exists a Lyapunov function $V(\boldsymbol{x})$, scalars $\alpha, \beta, p, q, k \in \mathbb{R}^+$, $pk < 1$, $gk > 1$, and $0 < \vartheta < \infty$, such that $\dot{V}(\boldsymbol{x}) \le -(\alpha V(\boldsymbol{x})^p + \beta V(\boldsymbol{x})^g)^k + \vartheta$. Then, the trajectory of this system is practical fixed-time stable. Moreover, the residual set of the solution of system (3) can be given by

$$\left\{ \lim_{t\to T} \boldsymbol{x} \,\middle|\, V(\boldsymbol{x}) \le \min\left\{ \alpha^{-1/p}\left(\frac{\vartheta}{1-\theta^k}\right)^{\frac{1}{kp}}, \beta^{-1/p}\left(\frac{\vartheta}{1-\theta^k}\right)^{\frac{1}{kg}} \right\} \right\}$$

where θ is a scalar and satisfies $0 < \theta \le 1$. The time needed to reach the residual set is bounded as $T \le (1/\alpha^k\theta^k(1-pk)) + (1/\beta^k\theta^k(gk-1))$.

Lemma 2 [17]: For any $x_i \in \mathbb{R}$, $(\sum_{i=1}^n |x_i|)^v \le \sum_{i=1}^n |x_i|^v$, where $v \in \mathbb{R}^+$ and $v \in (0, 1]$.

Lemma 3 [18]: If $v \in \mathbb{R}^+$ and $v > 1$, then for any $x, y \in \mathbb{R}$, we have $|x+y|^v \le 2^{v-1}|x^v + y^v|$.

III. New Fixed-Time-Based Sliding Mode Surface Design

A new fixed-time-based sliding mode (SM) surface, which explicitly considers the angular velocity information $\boldsymbol{\omega}$, is now proposed for spacecraft attitude stabilization. Existing TSM surfaces which explicitly contain $\boldsymbol{\omega}$ have been developed, for example $\boldsymbol{S} = \boldsymbol{\omega} + \alpha\text{sig}(\boldsymbol{q})^p$ [12] and $\boldsymbol{S} = \boldsymbol{\omega} + \alpha\text{sig}(\boldsymbol{q})^p + \beta\text{sig}(\boldsymbol{q})^g$ [16]. However, in both cases, a complete proof was not provided for the finite-time convergence after the states $\boldsymbol{q}$ and $\boldsymbol{\omega}$ arrive at their SM surface; the proofs are valid only for $q_0 \ge 0$. In the following, the fixed-time convergence of the proposed fixed-time-based SM will be proved and analyzed.

Considering the special characteristics of the spacecraft kinematics, a new fixed-time-based SM is given as

$$\boldsymbol{S} = \boldsymbol{\omega} + \boldsymbol{S_{au}} \tag{4}$$

where

$$S_{\text{aui}} = \begin{cases} \text{sig}[\alpha_1\text{sig}(q_i)^{p_1} + \beta_1\text{sig}(q_i)^{g_1}]^{k_1} \\ \qquad \text{if } \bar{S}_i = 0 \text{ or } \bar{S}_i \ne 0, \quad |q_i| > \varepsilon \\ l_1 q_i + l_2\text{sgn}(q_i)q_i^2 \\ \qquad \text{if } \bar{S}_i \ne 0, \quad |q_i| < \varepsilon \quad i = 1, 2, 3 \end{cases} \tag{5}$$

$$\bar{\boldsymbol{S}} = \boldsymbol{\omega} + \text{sig}(\alpha_1\text{sig}(\boldsymbol{q})^{p_1} + \beta_1\text{sig}(\boldsymbol{q})^{g_1})^{k_1} \tag{6}$$

where $\alpha_1, \beta_1, p_1, g_1$, and $k_1 > 0$ are the free design parameters, with $p_1 k_1 \in (0, 1)$ and $g_1 k_1 > 1$. $l_1 = (2-k_1)(\alpha_1\varepsilon^{p_1-1/k_1} + \beta_1\varepsilon^{g_1-1/k_1})^{k_1}$, $l_2 = (k_1-1)(\alpha_1\varepsilon^{p_1-2/k_1} + \beta_1\varepsilon^{g_1-2/k_1})^{k_1}$, and $\varepsilon > 0$ is a small constant.

Remark 1: The SM (6) is inspired by the sliding surface $\boldsymbol{S} = y_2 + \text{sig}[\text{sig}(y_2)^2 + \alpha_1 y_1 + \beta_1\text{sig}(y_1)^3]^{0.5}$ in [15],

Authorized licensed use limited to: CHONGQING UNIVERSITY. Downloaded on May 15,2023 at 10:16:32 UTC from IEEE Xplore. Restrictions apply.

with some differences. The biggest difference is that the angular velocity information $\boldsymbol{\omega}$ is explicitly considered in (5), so that the proposed SM has a clearer physical meaning.

Remark 2: The switching method (5) is inspired by [19] and [20] to avoid the singularity. The choice of l_1 and l_2 is to make the function $\boldsymbol{S_{au}}$ and its time derivative continuous. By choosing a small ε such that $|q_i| > \varepsilon$ as the fixed-time-based SM $\bar{\boldsymbol{S}}$ reaches zero, $\boldsymbol{q}$ and $\boldsymbol{\omega}$ will approach zero along the fixed-time-based SM [19].

Theorem 1: Consider spacecraft system (1) for the fixed-time-based SM (4) satisfying $\boldsymbol{S} = \bar{\boldsymbol{S}} = \boldsymbol{0}$. Then $\boldsymbol{q} = \boldsymbol{0}$, $q_0 = 1$, and $\boldsymbol{\omega} = \boldsymbol{0}$ can be reached in fixed-time T_q, without requiring any knowledge of the initial and instantaneous value of the system states. The fixed-time T_q satisfies

$$T_q < \frac{2}{\alpha_1}\bar{F}\left(\frac{1}{2}, (1+k_1p_1)/2; \frac{3}{2}; 1\right) + \frac{2^{(3+p_1k_1)/2}}{\alpha_1^{k_1}(1-p_1k_1)} + \frac{2^{(3+g_1k_1)/2}}{\beta_1^{k_1}(g_1k_1-1)} \tag{7}$$

where $\bar{F}(\cdot)$ is the Gauss' Hypergeometric function (see [21] for further details). Two evaluations of this function for reference are $\bar{F}(0.5, 0.6; 1.5; 1) \approx 1.8395$ and $\bar{F}(0.5, 0.8; 1.5; 1) \approx 3.1343$.

Proof: If the sliding motion occurs for system (4) such that $\boldsymbol{q}$ and $\boldsymbol{\omega}$ can be kept on the fixed-time-based SM, then $\boldsymbol{S} = \bar{\boldsymbol{S}} = \boldsymbol{0}$. That is, $\boldsymbol{\omega} = -\text{sig}[\alpha_1\text{sig}(\boldsymbol{q})^{p_1} + \beta_1\text{sig}(\boldsymbol{q})^{g_1}]^{k_1}$ and $\dot{q}_0 = -0.5\boldsymbol{q}^T\boldsymbol{\omega} = 0.5\boldsymbol{q}^T\text{sig}[\alpha_1\text{sig}(\boldsymbol{q})^{p_1} + \beta_1\text{sig}(\boldsymbol{q})^{g_1}]^{k_1}$. Let the positive definite Lyapunov function be of the form $V_q = \boldsymbol{q}^T\boldsymbol{q} + (1-q_0)^2 = 2(1-q_0)$. Taking the derivative of V_q yields

$$\begin{aligned}\dot{V}_q &= -2\dot{q}_0 = -\boldsymbol{q}^T\text{sig}[\alpha_1\text{sig}(\boldsymbol{q})^{p_1} + \beta_1\text{sig}(\boldsymbol{q})^{g_1}]^{k_1}\\ &= -|\alpha_1(\boldsymbol{q}^T\boldsymbol{q})^{(1/k_1+p_1)/2} + \beta_1(\boldsymbol{q}^T\boldsymbol{q})^{(1/k_1+g_1)/2}|^{k_1}.\end{aligned} \tag{8}$$

From the above analysis, it can be seen that, for $\dot{V}_q \le 0$, all of the states $\boldsymbol{q}$ will converge to the origin and $q_0 \in (-1, 1]$ will converge to 1. Next, we will prove that $\boldsymbol{q}$ and q_0 can stabilize the equilibrium in a finite time for two cases.

Case 1: If $q_0(T_S) \ge 0$, then one has $\dot{V}_q \le -(\alpha_1 0.5^{(1/k_1+p_1)/2}V_q^{(1/k_1+p_1)/2} + \beta_1 0.5^{(1/k_1+g_1)/2}V_q^{(1/k_1+g_1)/2})^{k_1}$. By Lemma 1, we have $T_{\text{qcase1}} \le (2^{(3+p_1k_1)/2}/\alpha_1^{k_1}(1-p_1k_1)) + (2^{(3+g_1k_1)/2}/\beta_1^{k_1}(g_1k_1-1))$.

Case 2: If $q_0(T_S) \in (-1, 0)$, then we choose the Lyapunov candidate function as $V_{|q0|} = |q_0|$. Its first-order derivative is

$$\begin{aligned}\dot{V}_{|q0|} &= -\frac{1}{2}\boldsymbol{q}^T\text{sig}[\alpha_1\text{sig}(\boldsymbol{q})^{p_1} + \beta_1\text{sig}(\boldsymbol{q})^{g_1}]^{k_1}\\ &= -\frac{1}{2}\left|\alpha_1(1-q_0^2)^{(1/k_1+p_1)/2} + \beta_1(1-q_0^2)^{(1/k_1+g_1)/2}\right|^{k_1}\\ &\le -\frac{1}{2}\alpha_1(1-V_{|q0|}^2)^{(1+k_1p_1)/2}.\end{aligned} \tag{9}$$

The fixed-time $T_{q0\to 0}$ can be obtained by integrating both sides of (9) to give

$$\begin{aligned}T_{q0\to 0} &\le \int_{V_{q0(T_S)}}^{0} -2/[\alpha_1(1-V_{q0}^2)^{(1+k_1p_1)/2}]dV_{q0(T_{S2})}\\ &< (2/\alpha_1)V_{q0}\bar{F}\left(0.5, (1+k_1p_1)/2; 1.5; V_{q0}^2\right)\Big|_{V_{q0}=1}\\ &= (2/\alpha_1)\bar{F}(0.5, (1+k_1p_1)/2; 1.5; 1).\end{aligned} \tag{10}$$

Thus, $q_0 = 0$ can be reached in fixed time $T_{q0\to 0}$. After time period $T_{q0\to 0}$, q_0 will converge from 0 to 1 in fixed time $T_{q0\to 1}$. Using the same approach as Case 1, $T_{q0\to 1}$ is given by $T_{q0\to 1} < (2^{(3+p_1k_1)/2}/\alpha_1^{k_1}(1-p_1k_1)) + (2^{(3+g_1k_1)/2}/\beta_1^{k_1}(g_1k_1-1))$.

Then, we have $T_{\text{qcase2}} = T_{q0\to 0} + T_{q0\to 1}$. Finally, combining the results for both cases T_{qcase1} and T_{qcase2} yields

$$\begin{aligned}T_q &= \max\{T_{\text{qcase1}}, T_{\text{qcase2}}\}\\ &< \frac{2}{\alpha_1}\bar{F}\left(\frac{1}{2}, \frac{(1+k_1p_1)}{2}; \frac{3}{2}; 1\right) + \frac{2^{(3+p_1k_1)/2}}{\alpha_1^{k_1}(1-p_1k_1)}\\ &\quad + \frac{2^{(3+g_1k_1)/2}}{\beta_1^{k_1}(g_1k_1-1)}.\end{aligned} \tag{11}$$

From (11), the bound of the convergence time T_{q2} can be estimated even if we have no knowledge of the initial and instantaneous values of the system states. Hence, the proof of Theorem 1 is completed.

IV. Fixed-Time-Based Finite-Time Controller Design

In this section, the fixed-time-based finite-time controller will be developed for spacecraft in the presence of external disturbances, actuator faults, and input saturation. To proceed with the design of the control scheme, the following reasonable assumptions are required.

Assumption 1: The external disturbance $\boldsymbol{d}(t)$ and the uncertain sticking failure $\bar{\boldsymbol{u}}$ in (1) are unknown but bounded. That is to say, there always exist positive but unknown constants d_{dist} and u_{stk} such that

$$\|\boldsymbol{D\sigma\bar{u}}\| + \|\boldsymbol{d}(t)\| \le d_{\text{dist}} + \|\boldsymbol{D}\|u_{\text{stk}} \triangleq \chi. \tag{12}$$

Assumption 2: The symmetric positive-definite inertia matrix is assumed to be unknown, but bounded by $\lambda_{\min}(\boldsymbol{J}) \parallel \boldsymbol{x} \parallel^2 \le \boldsymbol{x}^T\boldsymbol{J}\boldsymbol{x} \le \lambda_{\max}(\boldsymbol{J}) \parallel \boldsymbol{x} \parallel^2, \forall \boldsymbol{x} \in \mathbb{R}^3$, where $\lambda_{\max}(\cdot)$ and $\lambda_{\min}(\cdot)$ represent the minimum and maximum eigenvalues of a given matrix, respectively. Moreover, the failure indicators satisfy $E_i \ne 1$, and hence, $\lambda_{\min}(\boldsymbol{I}-\boldsymbol{E}) > 0$.

Combining (1) and the fixed-time-based SM (4), one has

$$\begin{aligned}\boldsymbol{J}\dot{\boldsymbol{S}} &= [\text{sig}(\alpha_1\text{sig}(\boldsymbol{q})^{p_1} + \beta_1\text{sig}(\boldsymbol{q})^{g_1})^{k_1} - \boldsymbol{S}]^{\times}\boldsymbol{J\omega}\\ &\quad + \boldsymbol{JW(q)Q(q)\omega} + \boldsymbol{D}(\boldsymbol{I}-\boldsymbol{\sigma})\Theta(\boldsymbol{u})\boldsymbol{u} + \boldsymbol{D\sigma\bar{u}} + \boldsymbol{d}(t)\end{aligned} \tag{13}$$

$$\boldsymbol{W(q)} = \begin{cases}\text{diag}(|\alpha_1\text{sig}(\boldsymbol{q})^{p_1} + \beta_1\text{sig}(\boldsymbol{q})^{g_1}|^{k_1-1})\\ \cdot[\alpha_1\text{diag}(|\boldsymbol{q}|^{p_1-1}) + \beta_1\text{diag}(|\boldsymbol{q}|^{g_1-1})]\\ \qquad\qquad \text{if } \bar{S}_i = 0 \text{ or } \bar{S}_i \ne 0,\ |q_i| > \varepsilon\\ l_1\boldsymbol{I_3} + 2l_2\text{diag}(\boldsymbol{q}) \quad \text{if } \bar{S}_i \ne 0, |q_i| < \varepsilon \quad i = 1, 2, 3.\end{cases} \tag{14}$$

Define an auxiliary variable Φ as

$$\Phi = [\text{sig}(\alpha_1\text{sig}(\boldsymbol{q})^{p_1} + \beta_1\text{sig}(\boldsymbol{q})^{g_1})^{k_1}]^{\times}\boldsymbol{J} + \boldsymbol{JW(q)Q(q)}. \tag{15}$$

From Assumption 2, $\|\boldsymbol{q}\| \le 1$, and $\|\boldsymbol{Q(q)}\| \le 1$, one has

$$\|\Phi\| = \lambda_{\max}(\boldsymbol{J})(\alpha_1+\beta_1)^{k_1} + \lambda_{\max}(\boldsymbol{J})\|\boldsymbol{W(q)}\ \boldsymbol{Q(q)}\| \le Y \tag{16}$$

where Y is an unknown and positive constant.

Authorized licensed use limited to: CHONGQING UNIVERSITY. Downloaded on May 15,2023 at 10:16:32 UTC from IEEE Xplore. Restrictions apply.

Remark 3: Note that, in the case that $\bar{S}_i \neq 0$, the fixed-time-based SM is switched into the general sliding manifold when q_i enters the region $|q_i| < \varepsilon$. So the singularity in (16) can be avoided in the case $\bar{S}_i \neq 0$. In addition, if $\boldsymbol{q}$ approaches a residual set, i.e., a region of zero, along the sliding manifold, then $\|\Phi\|$ is also bounded.

Theorem 2: Consider the spacecraft attitude system given in (1) with actuator faults, saturation, and disturbances satisfying Assumptions 1 and 2. The adaptive fixed-time-based finite-time controller

$$\boldsymbol{u} = -D^T[\alpha_2 \mathrm{sig}(\boldsymbol{S})^{p_2} + \beta_2 \boldsymbol{S}^{g_2} + \hat{\mu}(\hat{\chi} + \hat{Y}\|\omega\|)\mathrm{sign}(\boldsymbol{S})] \tag{17}$$

is proposed and updated by

$$\begin{aligned}\dot{\hat{\chi}} &= \frac{1}{2\theta_0 c_1}(\|\boldsymbol{S}\| - \sigma_1\hat{\chi}), \quad \dot{\hat{Y}} = \frac{1}{2\theta_0 c_2}(\|\boldsymbol{S}\|\|\boldsymbol{\omega}\| - \sigma_2\hat{Y})\\ \dot{\hat{\mu}} &= \frac{1}{2\theta_0 c_3}[\hat{\mu}^2\|\boldsymbol{S}\|(\hat{\chi} + \hat{Y}\|\boldsymbol{\omega}\|) + \sigma_3]\hat{\mu}\end{aligned} \tag{18}$$

where $\theta_0 \in (0,1)$ solves the equation $\theta_0^{(p_2+1/2)} + \theta_0 - 1 = 0$, $c_1 = \sigma_1(\theta_1 - 0.5)/\theta_1, c_2 = \sigma_2(\theta_2 - 0.5)/\theta_2$, and $c_3 = \sigma_3(\theta_3 - 0.5)/\theta_3$. $\alpha_2, \beta_2, \sigma_1, \sigma_2, \sigma_3, p_2,$ and $g_2 > 0$ are the controller parameters and satisfy $p_2 < 1$ and $g_2 > 1$. The adaptive values $\hat{\chi}$, $\hat{Y}$, and $\hat{\mu}$ are the estimates of the unknown parameters χ, Y, and μ, respectively, and μ satisfies $0 < \mu \leq \lambda_{\min}(\boldsymbol{D}(\boldsymbol{I}-\boldsymbol{E})\Theta(\boldsymbol{u})\boldsymbol{D}^T)$. Then, the trajectory of the closed-loop system will converge to a region in fixed time.

Proof: Substituting (12), (13), and (15) to (17) into $\boldsymbol{S}^T\boldsymbol{J}\dot{\boldsymbol{S}}$ yields

$$\begin{aligned}\boldsymbol{S}^T\boldsymbol{J}\dot{\boldsymbol{S}} &= \boldsymbol{S}^T\Phi\boldsymbol{\omega} + \boldsymbol{S}^T[\boldsymbol{D}(\boldsymbol{I}-\boldsymbol{\sigma})\Theta(\boldsymbol{u})\boldsymbol{u} + \boldsymbol{D}\boldsymbol{\sigma}\bar{\boldsymbol{u}} + \boldsymbol{d}(t)]\\ &\leq Y\|\boldsymbol{S}\|\|\omega\| + \chi\|\boldsymbol{S}\| + \boldsymbol{S}^T\boldsymbol{D}(\boldsymbol{I}-\boldsymbol{\sigma})\Theta(\boldsymbol{u})\boldsymbol{u}\\ &\leq Y\|\boldsymbol{S}\|\|\omega\| + \chi\|\boldsymbol{S}\| - \mu[\alpha_2\|\boldsymbol{S}\|^{p_2} + \beta_2\|\boldsymbol{S}\|\\ &\qquad + \hat{\mu}(\hat{\chi} + \hat{Y}\|\boldsymbol{\omega}\|)]\|\boldsymbol{S}\|\\ &\leq -\mu\alpha_2\|\boldsymbol{S}\|^p\|\boldsymbol{S}\| - \mu\beta_2\|\boldsymbol{S}\|^2 - \mu\hat{\mu}\hat{\chi}\|\boldsymbol{S}\|\\ &\quad - \mu\hat{\mu}\hat{Y}\|\boldsymbol{S}\|\|\boldsymbol{\omega}\| + Y\|\boldsymbol{S}\|\|\boldsymbol{\omega}\| + \chi\|\boldsymbol{S}\|.\end{aligned} \tag{19}$$

Considering the Lyapunov candidate function $V_S = (1/2)\boldsymbol{S}^T\boldsymbol{J}\boldsymbol{S} + \theta_0(c_1\tilde{\chi}^2 + c_2\tilde{Y}^2 + c_3\tilde{\mu}^2)$ and taking the derivative give

$$\begin{aligned}\dot{V}_S &= \boldsymbol{S}^T\boldsymbol{J}\dot{\boldsymbol{S}} - 2\theta_0 c_1\tilde{\chi}\dot{\hat{\chi}} - 2\theta_0 c_1\tilde{Y}\dot{\hat{Y}} + 2\theta_0 c_1\tilde{\mu}\hat{\mu}^{-2}\dot{\hat{\mu}}\\ &\leq -\mu a_2\|\boldsymbol{S}\|^{p_2}\|\boldsymbol{S}\| - \mu\beta_2\|\boldsymbol{S}\|^{g_2}\|\boldsymbol{S}\|\\ &\quad + \sigma_1\tilde{\chi}\hat{\chi} + \sigma_2\tilde{Y}\hat{Y} + \sigma_3\tilde{\mu}\hat{\mu}^{-1}.\end{aligned} \tag{20}$$

For any $\theta_1 > (1/2)$, $\theta_2 > (1/2)$, and $\theta_3 > (1/2)$, one has

$$\sigma_1\tilde{\chi}\hat{\chi} = -\sigma_1\tilde{\chi}(\tilde{\chi} - \chi) \leq -c_1\tilde{\chi}^2 + \frac{\theta_1\sigma_1}{2}\chi^2 \tag{21}$$

$$\sigma_2\tilde{Y}\hat{Y} = -\sigma_2\tilde{Y}(\tilde{Y} - Y) \leq -c_2\tilde{Y}^2 + \frac{\theta_2\sigma_2}{2}Y^2 \tag{22}$$

$$\sigma_3\tilde{\mu}\hat{\mu}^{-1} = -\sigma_3\tilde{\mu}(\tilde{\mu} - \mu) \leq -c_3\tilde{\mu}^2 + \frac{\theta_3\sigma_3}{2}\mu^2. \tag{23}$$

Substituting (21) to (23) into (14) and further simplification yield

$$\begin{aligned}&\dot{V}_S\\ &\leq -\mu a_2\|\boldsymbol{S}\|^{p_2+1} - \mu\beta_2\|\boldsymbol{S}\|^{g_2+1} + \sigma_1\tilde{\chi}\hat{\chi} + \sigma_2\tilde{Y}\hat{Y} + \sigma_3\tilde{\mu}\hat{\mu}^{-1}\\ &\leq -\eta_1 V_S^{(p_2+1)/2} - 2^{1-g_1}\eta_2 V_S^{(g_2+1)/2} + \vartheta_1 + (\theta_0 c_1\tilde{\chi}^2)^{(g_2+1)/2}\\ &\quad + (\theta_0 c_2\tilde{Y}^2)^{(g_2+1)/2} + (\theta_0 c_3\tilde{\mu}^2)^{(g_2+1)/2} - \theta_0 c_1\tilde{\chi}^2\\ &\quad - \theta_0 c_2\tilde{Y}^2 - \theta_0 c_3\tilde{\mu}^2\end{aligned} \tag{24}$$

where

$$\begin{aligned}\eta_1 &= \min\{\mu\alpha_2/\{[(1/2)\lambda_{\max}(\boldsymbol{J})]^{(p_2+1)/2}\}, 1\}\\ \eta_2 &= \min\{\mu\beta_2/\{[(1/2)\lambda_{\max}(\boldsymbol{J})]^{(p_2+1)/2}\}, 1\}\\ \vartheta_1 &= \frac{\sigma_1\theta_1}{2}\chi^2 + \frac{\sigma_2\theta_2}{2}Y^2 + \frac{\sigma_3\theta_3}{2}\mu^2 + 3\theta_0^{\frac{p_2+1}{2}}\vartheta_0\end{aligned}$$

$\vartheta_0 = p_0^{p_0/(1-p_0)} - p_0^{1/(1-p_0)} > 0$ and $p_0 = (p_2+1)/2$. Moreover, assume that there exists an unknown constant Δ and a compact set D such that $D = \{(\tilde{\chi}, \tilde{Y}, \tilde{\mu}) | \tilde{\chi} \leq \Delta, \tilde{Y} \leq \Delta, \tilde{\mu} \leq \Delta\}$. Then we have

$$\dot{V}_S \leq -\eta_1 V_S^{(p_2+1)/2} - 2^{1-g_2}\eta_2 V_S^{(g_2+1)/2} + \vartheta \tag{25}$$

where

$$\vartheta = \begin{cases}\vartheta_1 & \text{if } \Delta \leq \min\{1/\sqrt{\theta_0 c_1}, 1/\sqrt{\theta_0 c_2}, 1/\sqrt{\theta_0 c_3}\}\\ \vartheta_1 + 3(\theta_0 c_{\max}\Delta^2)^{\frac{g_2+1}{2}} - 3\theta_0 c_{\max}\Delta^2 & \\ & \text{if } \Delta \geq \min\{1/\sqrt{\theta_0 c_1}, 1/\sqrt{\theta_0 c_2}, 1/\sqrt{\theta_0 c_3}\}\end{cases}$$

and $c_{\max} = \max\{c_i\}$.

From Lemma 1, the trajectory of the system in (1) tends to be practical fixed-time stable. Moreover, the residual set D_1 is calculated as $D_1 = \{\lim_{t\to T_{S2}} \boldsymbol{S}(t) | V_S \leq \min\{[(\vartheta/\eta_1(1-\theta))]^{2/(p_2+1)}, [(2^{g_1-1}\vartheta/\eta_2(1-\theta))]^{2/(g_2+1)}\}\}$ and the settling time T_{S1} is given by $T_{S1} \leq 1/[\eta_1\theta(1-p_2)] + 2^{g_2-1}/[\eta_2\theta(g_2-1)]$. Hence, the proof of Theorem 2 is completed.

Remark 4: Note that the expression of the proposed controller (17) has a switching term $\hat{\mu}(\hat{\chi} + \hat{Y}\|\omega\|)$ sign $(\boldsymbol{S})$, whose magnitude (i.e., $\hat{\mu}(\hat{\chi} + \hat{Y}\|\omega\|)$) depends on the adaptive laws (18). Through the above proof, we know that the switching term $\hat{\mu}(\hat{\chi} + \hat{Y}\|\omega\|)\mathrm{sign}(\boldsymbol{S})$ can counteract system model uncertainties. Thus, a larger disturbance, a smaller saturation degree coefficient $\Theta_i(u_i)$, or a smaller failure coefficient E_i will require a larger magnitude $\hat{\mu}(\hat{\chi} + \hat{Y}\|\omega\|)$.

V. Simulation Results and Comparison

To verify the effectiveness of the proposed fixed-time-based sliding surface and controllers, the detailed responses are numerically simulated using the rigid spacecraft system governed by (1) in conjunction with the proposed adaptive fixed-time controller in (17), the finite-time controller in [23], and a proportional–derivative (PD) controller. The inertia matrix is taken as $\boldsymbol{J} = [20, 1.2, 0.9; 1.2, 17, 1.4; 0.9, 1.4, 15]$ kg · m^2. To improve the reliability of the attitude control system, four reaction wheels are mounted on the spacecraft in a tetrahedron configuration [22], and the configuration

Authorized licensed use limited to: CHONGQING UNIVERSITY. Downloaded on May 15,2023 at 10:16:32 UTC from IEEE Xplore. Restrictions apply.

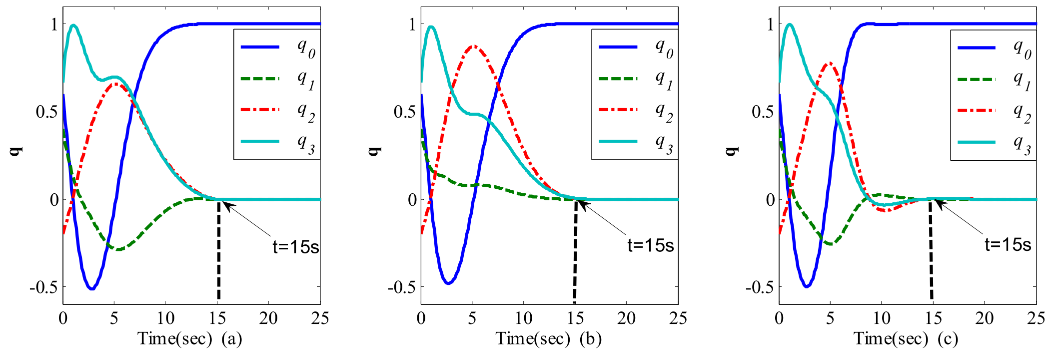

Fig. 1. Time response of attitude $\boldsymbol{q}$ with healthy actuators. (a) Adaptive fixed-time-based finite-time controller in (17). (b) Finite-time controller in [23]. (c) PD controller.

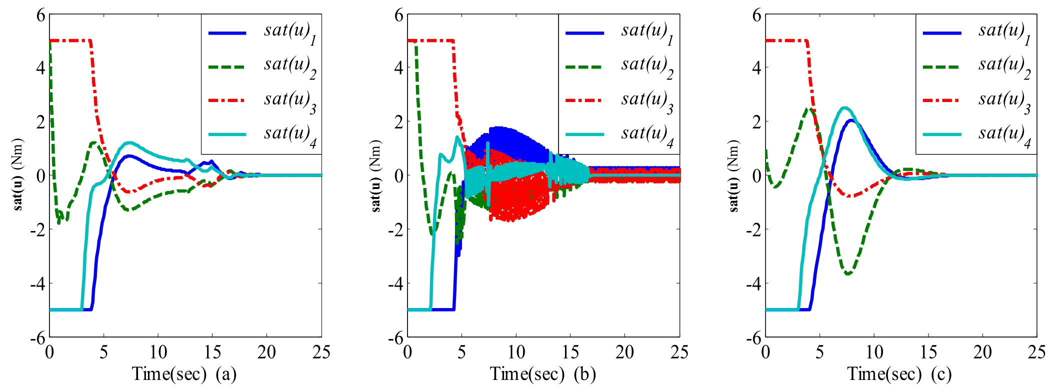

Fig. 2. Time response of attitude sat($\boldsymbol{u}$) with healthy actuators. (a) Adaptive fixed-time-based finite-time controller in (17). (b) Finite-time controller in [23]. (c) PD controller.

matrix is defined as

$$\boldsymbol{D} = \left[\frac{1}{\sqrt{3}}, \frac{1}{\sqrt{3}}, -\frac{1}{\sqrt{3}}, -\frac{1}{\sqrt{3}}; \sqrt{\frac{2}{3}}, -\sqrt{\frac{2}{3}}, 0, 0; 0, 0, -\sqrt{\frac{2}{3}}, \sqrt{\frac{2}{3}}\right].$$

The limited control torque of each reaction wheel is $\tau_{\max,i} = 5$ Nm. The external disturbance $\boldsymbol{d}(t)$ is taken into account and chosen as $\boldsymbol{d} = [3\cos(0.2t); 1.5\sin(0.2t) + 2; 3\sin(t)] \times 10^{-3}$ Nm. The initial conditions have been set to $[q_0, \boldsymbol{q}^T] = [0.6, 0.4, -0.2, 0.6633]$ and $\boldsymbol{\omega}(0) = [0.5; 1; 1.5]$. In addition, it is assumed that the attitude measurements are corrupted with random measurement noise of magnitude 0.05 deg per second. Although, in practice, noisy measurements are first filtered using a suitable filter before being used to calculate the control law, raw measurements are used here to demonstrate the robustness of the controller.

For the purposes of comparison, the developed controllers are compared with the finite-time controller in [23] and PD control with the same initial conditions. Because the finite-time controller and PD control do not consider actuator saturation, for fair comparison purposes, the abrupt saturation of this brief will be applied to the controllers.

Case A (Comparison With Healthy Actuators): In order to make a one-to-one comparison, the parameters have been set in such a way that they ensure that the settling times for the attitude for the three controllers are identical. Selected by trial and error until a good tracking performance is obtained, the control gains for the three controllers are as follows: fixed-time-based finite-time controller parameters are $\alpha_1 = \beta_1 = 0.7$, $p_1 = p_2/2 = 0.4$, $g_1 = g_2/2 = 1.5$, $k_1 = 2$, $\alpha_2 = \beta_2 = 10$, $c_i = 1$, $\sigma_i = 10$, $\hat{\chi}(0) = \hat{Y}(0) = \hat{\mu}(0) = 0.01$, and $\varepsilon = 0.005$; finite-time controller parameters are $k_1 = 5$, $k_2 = 0.75$, and $p = 1.3$; and PD controller parameters are $kp = 15$ and $kd = 13$. Note that α_i, β_i, p_i, and g_i mainly influence the convergence rate, and c_i and σ_i mainly influence the adaptive law (i.e., fault tolerant capability and robustness to external disturbances). The comparative simulations are conducted and the results are shown in Figs. 1 and 2. Fig. 1 shows that the settling times for the attitude for all the three controllers are indeed identical, i.e., 15 s. Fig. 2 shows that the actual control torques are within their maximum allowable limits, i.e., 5 Nm. It can be seen that the finite-time controller in [23] has significant chattering.

Case B (Comparison With Actuator Faults): In this case, severe actuator faults are considered, and the fault scenario is given by

$$E_1 = \begin{cases} 1, & \text{if } t \le 3.5 \\ 0.2, & \text{otherwise} \end{cases} \quad E_2 = \begin{cases} 1, & \text{if } t \le 5.5 \\ 0.4, & \text{otherwise} \end{cases} \quad E_3 = 0$$
$$E_4 = \begin{cases} 1, & \text{if } t \le 7 \\ 0.6, & \text{otherwise} \end{cases} \tag{26}$$

$$\bar{u}_1 = \bar{u}_3 = \bar{u}_4 = 0, \quad \bar{u}_2 = \begin{cases} 0.1, & \text{if } t \le 8 \\ 0, & \text{otherwise.} \end{cases} \tag{27}$$

Authorized licensed use limited to: CHONGQING UNIVERSITY. Downloaded on May 15,2023 at 10:16:32 UTC from IEEE Xplore. Restrictions apply.

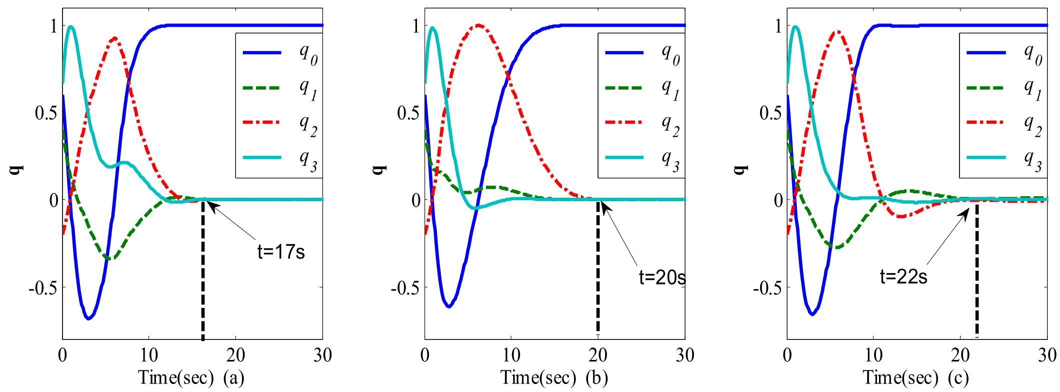

Fig. 3. Time response of attitude $\boldsymbol{q}$ with faulty actuators. (a) Adaptive fixed-time-based finite-time controller in (17). (b) Finite-time controller in [23]. (c) PD controller.

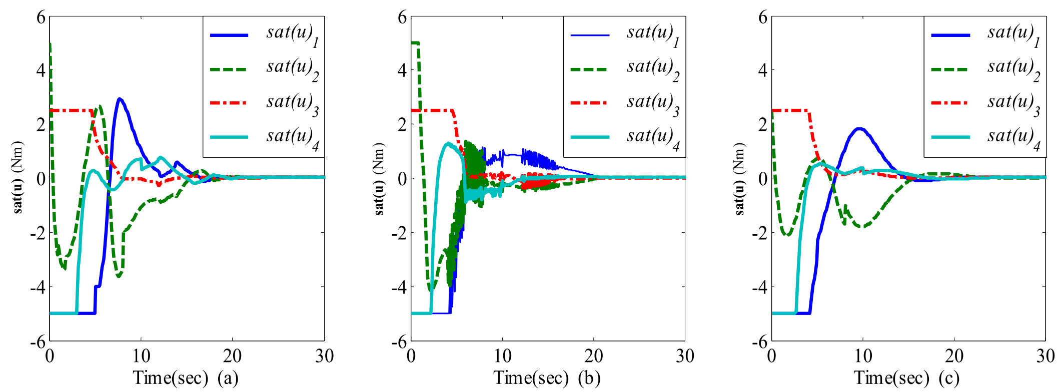

Fig. 4. Time response of attitude sat($\boldsymbol{u}$) with faulty actuators. (a) Adaptive fixed-time-based finite-time controller in (17). (b) Finite-time controller in [23]. (c) PD controller.

In addition, we also consider uncertain inertia where the variation of the inertia moments is less than 8%. The control parameters remain the same as given in Case A, and the results are shown in Figs. 3 and 4. Fig. 3 shows the time response of attitude for the three controllers, and it is clear that the proposed fixed-time-based finite-time controller has the fastest transient response with the highest accuracy. The system performance is significantly degraded for the PD controller. Fig. 4 shows the actual control torques and we can see that the finite-time controller in [23] still has serious oscillations, as in Case A. This case demonstrates the desirable features of the proposed fixed-time-based finite-time controller, such as finite-time convergence, fault tolerant capability, and robustness to external disturbances and uncertain inertia parameters.

Summarizing all the cases, it is noted that the proposed scheme can successfully accomplish attitude stabilization with high attitude pointing accuracy and stability in the presence of external disturbances, measurement noise, wheel faults, and even actuator input constraints in both theory and simulations. In addition, extensive simulations were also performed using different control parameters, disturbance inputs, and even combinations of the actuator output limit. These results show that the closed-loop system attitude stabilization is accomplished in spite of these undesired effects in the system. Moreover, the flexibility in the choice of control parameters can be utilized to obtain the desired performance while meeting the constraints on the control magnitude.

VI. Conclusion

A fixed-time-based finite-time control scheme for spacecraft attitude stabilization is developed with actuator faults and actuator saturation. In contrast to the existing finite-time control literature, the fixed-time-based finite-time control scheme is independent of initial conditions and has a more rapid convergence and higher pointing accuracy. The performance of the proposed fixed-time-based finite-time controller was examined through numerical simulation of the governing nonlinear system equations of motion and was compared with a traditional finite-time controller. The simulation showed that the proposed fixed-time control scheme can provide faster convergence and better fault-tolerance capability with higher accuracy than the existing controller. In future work, the extension of the fixed-time-based finite-time controller to output feedback control design will be investigated.

References

[1] H. Alwi and C. Edwards, "Fault tolerant control using sliding modes with on-line control allocation," *Automatica*, vol. 44, no. 7, pp. 1859–1866, Jul. 2008.
[2] Y.-W. Liang, S.-D. Xu, and C.-L. Tsai, "Study of VSC reliable designs with application to spacecraft attitude stabilization," *IEEE Trans. Control Syst. Technol.*, vol. 15, no. 2, pp. 332–338, Mar. 2007.
[3] Q. Hu, "Robust adaptive sliding-mode fault-tolerant control with L_2-gain performance for flexible spacecraft using redundant reaction wheels," *IET Control Theory Appl.*, vol. 4, no. 6, pp. 1055–1070, Jun. 2010.
[4] Q. Hu, "Adaptive output feedback sliding-mode manoeuvring and vibration control of flexible spacecraft with input saturation," *IET Control Theory Appl.*, vol. 2, no. 6, pp. 467–478, Jun. 2008.

Authorized licensed use limited to: CHONGQING UNIVERSITY. Downloaded on May 15,2023 at 10:16:32 UTC from IEEE Xplore. Restrictions apply.

[5] K. Lu, Y. Xia, and M. Fu, "Controller design for rigid spacecraft attitude tracking with actuator saturation," *Inf. Sci.*, vol. 220, pp. 343–366, Jan. 2013.

[6] R. J. Wallsgrove and M. R. Akella, "Globally stabilizing saturated attitude control in the presence of bounded unknown disturbances," *J. Guid., Control, Dyn.*, vol. 28, no. 5, pp. 957–963, 2005.

[7] Q. Hu, "Robust adaptive sliding mode attitude maneuvering and vibration damping of three-axis-stabilized flexible spacecraft with actuator saturation limits," *Nonlinear Dyn.*, vol. 55, no. 4, pp. 301–321, Mar. 2009.

[8] S. P. Bhat and D. S. Bernstein, "Finite-time stability of continuous autonomous systems," *SIAM J. Control Optim.*, vol. 38, no. 3, pp. 751–766, Jan. 2000.

[9] S. P. Bhat and D. S. Bernstein, "Geometric homogeneity with applications to finite-time stability," *Math. Control, Signals, Syst.*, vol. 17, no. 2, pp. 101–127, Jun. 2005.

[10] S. P. Bhat and D. S. Bernstein, "Continuous finite-time stabilization of the translational and rotational double integrators," *IEEE Trans. Autom. Control*, vol. 43, no. 5, pp. 678–682, May 1998.

[11] S. Wu, G. Radice, Y. Gao, and Z. Sun, "Quaternion-based finite time control for spacecraft attitude tracking," *Acta Astron.*, vol. 69, nos. 1–2, pp. 48–58, Jul./Aug. 2011.

[12] Q. Hu, X. Huo, B. Xiao, and Z. Zhang, "Robust finite-time control for spacecraft attitude stabilization under actuator fault," *Proc. Inst. Mech. Eng. I, J. Syst. Control Eng.*, vol. 226, no. 3, pp. 416–428, Mar. 2012.

[13] Q. Hu, X. Huo, and B. Xiao, "Reaction wheel fault tolerant control for spacecraft attitude stabilization with finite-time convergence," *Int. J. Robust Nonlinear Control*, vol. 23, no. 15, pp. 1737–1752, Oct. 2013.

[14] K. Lu and Y. Xia, "Finite-time fault-tolerant control for rigid spacecraft with actuator saturations," *IET Control Theory Appl.*, vol. 7, no. 11, pp. 1529–1539, Jul. 2013.

[15] A. Polyakov, "Nonlinear feedback design for fixed-time stabilization of linear control systems," *IEEE Trans. Autom. Control*, vol. 57, no. 8, pp. 2106–2110, Aug. 2012.

[16] Z. Zhu, Y. Xia, and M. Fu, "Attitude stabilization of rigid spacecraft with finite-time convergence," *Int. J. Robust Nonlinear Control*, vol. 21, no. 6, pp. 686–702, Apr. 2011.

[17] C. Qian and W. Lin, "A Continuous feedback approach to global strong stabilization of nonlinear systems," *IEEE Trans. Autom. Control*, vol. 46, no. 7, pp. 1061–1079, Jul. 2001.

[18] L. Ji, C. Qian, and M. T. Frye, "A dual-observer design for global output feedback stabilization of nonlinear systems with low-order and high-order nonlinearities," *Int. J. Robust Nonlinear Control*, vol. 19, no. 15, pp. 1697–1720, Oct. 2009.

[19] L. Wang, T. Chai, and L. Zhai, "Neural-network-based terminal sliding-mode control of robotic manipulators including actuator dynamics," *IEEE Trans. Ind. Electron.*, vol. 56, no. 9, pp. 3296–3394, Sep. 2009.

[20] K. Lu and Y. Xia, "Adaptive attitude tracking control for rigid spacecraft with finite-time convergence," *Automatica*, vol. 49, no. 12, pp. 3591–3599, 2013.

[21] M. Abramowitz and I. A. Stegun, *Handbook of Mathematical Functions: With Formulas, Graphs, and Mathematical Tables*. New York, NY, USA: Dover, 1965.

[22] B. Bialke, "High fidelity mathematical modeling of reaction wheel performance," in *Proc. 21st Annu. AAS Rocky Mountain Guid. Control Conf.*, Breckenridge, CO, USA, 1998, pp. 483–496.

[23] H. Du, S. Li, and C. Qian, "Finite-time attitude tracking control of spacecraft with application to attitude synchronization," *IEEE Trans. Autom. Control*, vol. 56, no. 11, pp. 2711–2717, Nov. 2011.

Authorized licensed use limited to: CHONGQING UNIVERSITY. Downloaded on May 15,2023 at 10:16:32 UTC from IEEE Xplore. Restrictions apply.